JPET Fast Forward. Published on July 7, 2006 as DOI: 10.1124/jpet.106.104521

JPET #104521

Discovery of pyrrolo[2,3-*b*]pyrazines derivatives as submicromolar affinity activators of wild-type, G551D and F508del CFTR chloride channels

Sabrina Noel, Christelle Faveau, Caroline Norez, Christian Rogier, Yvette Mettey, Frédéric Becq

Institut de Physiologie et Biologie Cellulaires CNRS UMR 6187, Université de Poitiers, 40 avenue du recteur Pineau 86022 Poitiers, France (S.N., C.F., C.N., C.R., Y.M., F.B.).

Faculté de Médecine et Pharmacie, BP 199, 34 Rue du Jardin des Plantes, 86005 Poitiers cedex, France (C.F., Y.M.).

Running title: pyrrolo[2,3-*b*]pyrazines activators of CFTR

Address correspondence to: Pr. Frédéric Becq, IPBC CNRS UMR 6187, Université de Poitiers, 40 Avenue du Recteur Pineau 86022 Poitiers, France. E-mail: frederic.becq@univ-poitiers.fr

33 text pages

1 table

9 figures

38 refs

Abstract: 247 words

Introduction: 452 words

Discussion: 1046 words

Nonstandard abbreviations: CDK: cyclin-dependent kinase, CF: cystic fibrosis, CFTR: cystic fibrosis transmembrane conductance regulator, $CFTR_{inh}$-172: 3-[(3-trifluoromethyl)phenyl]-5-[(4-carboxyphenyl)methylene]-2-thioxo-4-thiazolidinone, CHO: chinese hamster ovary, DIDS: 4,4′-diisothiocyanatostilbene-2,2′-disulfonic acid, DMSO: dimethyl sulfoxide, ENaC: epithelial sodium channel, fsk: forskolin, GSK-3: glycogen synthase kinase-3, Gst: genistein, Isc: short-circuit current, k_{basal}: basal rate of efflux, k_{peak}: peak rate of efflux, RP-107: 7-*n*-butyl-6-(4-hydroxyphenyl)[5*H*]pyrrolo[2,3-*b*]pyrazine, RP-108: 7-*n*-butyl-6-(4-chlorophenyl)[5*H*]pyrrolo[2,3-*b*]pyrazine, R_{TE}: transepithelial resistance, TES: (N-tris[hydroxymethyl]methyl-2-aminoethane-sulfonic acid, TS-TM calix[4]arene: 5,11,17,23-tetrasulfonato-25,26,27,28-tetramethoxy-calix[4]arene, V_{TE}: transepithelial potential difference, wt: wild-type.

Recommended section: cellular and molecular

Abstract

The cystic fibrosis transmembrane conductance regulator (CFTR) represents the main Cl^- channel in the apical membrane of epithelial cells for cAMP-dependent Cl^- secretion. Here we report on the synthesis and screening of a small library of 6-phenylpyrrolo[2,3-*b*]pyrazines (named RP derivatives) evaluated as activators of wild-type CFTR, G551D-CFTR and F508del-CFTR Cl^- channels. Iodide efflux and whole-cell patch clamp recordings analysis identified RP-107 as a submicromolar activator of wt-CFTR (human airway epithelial Calu-3 and wtCFTR-CHO cells), G551D-CFTR (G551D-CFTR-CHO cells) and F508del-CFTR (in temperature corrected human airway epithelial F508del/F508del CF15 cells). The structural analogue RP-108 (4-chlorophenyl), contrary to RP-107 (4-hydroxyphenyl), was less potent being activator only at micromolar concentrations. RP-107 and RP-108 did not have any effect on the cellular cAMP level. Activation was potentiated by low concentration of forskolin and inhibited by glibenclamide and $CFTR_{inh}$-172 but not by calixarene or DIDS. Finally, we found significant stimulation of short circuit current (Isc) by RP-107 (EC_{50} = 89 nM) and RP-108 (EC_{50} = 103 μM) on colon of *Cftr*$^{+/+}$ but not of *Cftr*$^{-/-}$ mice mounted in Ussing chamber. Stimulation of Isc was inhibited by glibenclamide but not affected by DIDS. These results show that RP-107 stimulates wild-type CFTR and mutated CFTR, with submicromolar affinity by a cAMP-independent mechanism. Our preliminary structure-activity relationship study identified 4-hydroxyphenyl and 7-*n*-butyl as determinants required for activation of CFTR. The potency of these agents indicates that compounds in this class may be of therapeutic benefit in CFTR-related diseases, including cystic fibrosis.

Introduction

Cystic Fibrosis (CF) is a worldwide fatal autosomal recessive genetic disease caused by mutations in the *CFTR* gene (Riordan et al., 1989; Ratjen & Doring, 2003). CF affects 1/2500 to 1/3500 live births with an estimated global CF population above 70,000 individuals. Mutations in the *cystic fibrosis transmembrane conductance regulator* (*CFTR*) gene alter composition of epithelial secretions and lead to chronic airway obstructions and infections, pancreatic failure, male infertility, and elevated level of salt in sweat (Quinton, 1983; Riordan et al., 1989; Ratjen & Doring, 2003). CFTR functions as a cyclic AMP-dependent and ATP-gated Cl^- channel (Anderson et al., 1991; Tabcharani et al., 1991; Sheppard & Welsh, 1999) and is thought to be the main cAMP-dependent pathway for Cl^- exit and hence for fluid secretion in epithelial cells in the airways, pancreas, intestine, testis and other fluid-transporting tissues (Gray et al., 1988; Shen et al., 1994; Sheppard & Welsh, 1999; Ratjen & Doring, 2003). Individuals suffering from CF often require frequent hospitalizations and heavy medication. Although these treatments do not cure the disease, they have allowed the median age of survival to rise from 14 years in 1969 to ≈35 nowadays and also improved the physical comfort and social life of CF patients (http://www.cff.org). More than 1300 mutations of the CF gene have been so far detected via worldwide chromosome analysis (http://www.genet.sickkids.on.ca/cftr). Due to this large number of gene abnormalities, CFTR mutations were assigned according to the fate of the final product into one of six classes of mutations (Welsh and Smith, 1993). Based on this classification it is therefore feasible to predict the strategy for developing a CF therapy according to the class of the CFTR mutation.

Identification of a selective agonist for a particular ion channel without secondary effect on other channels or unrelated proteins is critical for use as a biological tool or

pharmaceutical drug but is a high-cost process that usually takes several years. However, a number of compounds have been identified during the last 15 years activating wild-type and mutated CFTR by mechanisms that do not involve an increase of intracellular cAMP (reviewed in Becq, 2006). Our laboratory develops, synthesizes original small molecules and evaluates them for their ability to activate CFTR using a simple and robust robotic cell-based assay (Marivingt-Mounir et al., 2004). In this report we present the 6-phenylpyrrolo[2,3-*b*]pyrazines, a family of derivatives (also named Aloisines) initially described as CDK/GSK-3 inhibitors (Mettey et al., 2003). One of these compounds, RP-107 activates CFTR dependent Cl^- secretion with submicromolar affinity in various epithelial cell types. Moreover, RP-107 activates two CF-associated CFTR mutants (G551D-CFTR and F508del-CFTR mutants). The potency of these agents indicates the possibility that compounds in this class may be of therapeutic benefit in CF.

JPET Fast Forward. Published on July 7, 2006 as DOI: 10.1124/jpet.106.104521
This article has not been copyedited and formatted. The final version may differ from this version.

Materials and methods

Chemistry

The 6-phenylpyrrolo[2,3-*b*]pyrazines derivatives shown in Table 1 were synthesized as presented in figure 1, from alkylpyrazines and aromatic nitriles, as previously described (Vierfond et al., 1981). Demethylation of methoxycompounds (1, 3, 5, 7 and 9) was obtained by heating in refluxing HBr. Synthesis and spectral data of compounds 1-8 and 11-12 (Table 1) are described elsewhere (Mettey et al., 2003).

Compounds used are: 6-(4-methoxyphenyl)[5*H*]pyrrolo[2,3-*b*]pyrazine (**1**, RP11), 6-(4-hydroxyphenyl)[5*H*]pyrrolo[2,3-*b*]pyrazine (**2**, RP26), 6-(4-methoxyphenyl)-7-methyl[5*H*]pyrrolo[2,3-*b*]pyrazine (**3**, RP95), 6-(4-hydroxyphenyl)-7-methyl[5*H*]pyrrolo[2,3-*b*]pyrazine (**4**, RP96), 6-(4-methoxyphenyl)-7-propyl[5*H*]pyrrolo[2,3-*b*]pyrazine (**5**, RP127), 6-(4-hydroxyphenyl)-7-propyl[5*H*]pyrrolo[2,3-*b*]pyrazine (**6**, RP132), 7-*n*-butyl-6-(4-methoxyphenyl)[5*H*]pyrrolo[2,3-*b*]pyrazine (**7**, RP106), 7-*n*-butyl-6-(4-hydroxyphenyl)[5*H*]pyrrolo[2,3-*b*]pyrazine (**8**, RP107), 6-(4-chlorophenyl)[5*H*]pyrrolo[2,3-*b*]pyrazine (**11**, RP14), 7-*n*-butyl-6-(4-chlorophenyl)[5*H*]pyrrolo[2,3-*b*]pyrazine (**12**, RP108).

Similar chemical synthesis method has been used for compounds 9 and 10. The corresponding elemental analysis are provided below.

*7-n-pentyl-6-(4-methoxyphenyl)[5H]pyrrolo[2,3-b]pyrazine (**9**, RP149)*: m.p. 144.2°C; IR 3143, 3059, 2959, 2927, 2858 cm^{-1}; ^1H NMR (60 MHz, DMSO-d_6), δ 11.75 (bs, 1H), 8.40 and 8.20 (2d, 1H each, J = 2.6 Hz), 7.70 and 7.10 (2bd, 2H each, J = 8 Hz), 3.90 (s, 3H), 3.20-2.80 (m, 2H), 2.00-1.1 (m, 6H), 0.9 (t, 3H, J = 7.2 Hz). Anal. Calcd for $C_{18}H_{21}N_3O$ (295.39) Calcd for $C_{18}H_{21}N_3O$: C, 73.19; H, 7.17; N, 14.22. Found: C, 73.06; H, 7.26; N, 14.09.

*7-n-pentyl-6-(4-hydroxyphenyl)[5H]pyrrolo[2,3-b]pyrazine (**10**, RP150):* m.p. 270.7°C. IR 3224, 3150, 3060, 2949, 2924, 2861 cm^{-1}. ^1H NMR (60 MHz, DMSO-d_6) δ 11.85 (bs, 1H),

JPET Fast Forward. Published on July 7, 2006 as DOI: 10.1124/jpet.106.104521
This article has not been copyedited and formatted. The final version may differ from this version.

9.90 (bs, 1H), 8.35 and 8.15 (2d, 1H each, J = 2.6 Hz), 7.50 and 6.95 (2d, 2H each, J = 7 Hz), 3.10-1.70 (m, 2H), 2.00-1.05 (m, 6H), 0.80 (t, 3H, J = 7 Hz). Anal. Calcd for $C_{17}H_{19}N_3O$ (281.36): C, 72.57; H, 6.81; N, 14.93. Found: C, 72.35; H, 6.78; N, 14.75.

Other chemicals. TS-TM calix[4]arene (5,11,17,23-tetrasulfonato-25,26,27,28-tetramethoxy-calix[4]arene) an inhibitor of outwardly rectifying Cl^- channels (Singh et al., 1995) was generously provided by Drs Singh and Bridges, University of Pittsburgh, Pittsburgh, USA. The specific CFTR inhibitor 3-[(3-trifluoromethyl)phenyl]-5-[(4-carboxyphenyl)methylene]-2-thioxo-4-thiazolidinone ($CFTR_{inh}$-172) (Ma et al., 2002), and forskolin were purchased from Calbiochem (VWR international, Fontenay/bois, France) and LC laboratory (PKC Pharmaceuticals, Inc, Woburn, MA, USA), respectively. All other chemicals were from Sigma (St Louis, MO, USA). All chemical agents including pyrrolo[2,3-*b*]pyrazines compounds were dissolved in dimethylsulfoxide DMSO (Me_2SO, final concentration ≤ 0.1%), except TS-TM calix[4]arene, which was dissolved in H_2O. The current were not altered by Me_2SO alone.

Cell culture. All cell lines were grown at 37°C in 5% CO_2 under standard culture conditions, as follow. CHO cells stably transfected with pNUT vector alone (mock-CHO) or containing wild-type CFTR (wtCFTR-CHO) and the mutant G551D-CFTR were provided by J.R. Riordan and X.B. Chang, Scottsdale, AZ, USA (Tabcharani et al., 1991; Becq et al., 1994; Becq et al., 1999). They were maintained in αMEM-GlutaMAX containing 7% FBS, 50 IU/mL penicillin and 50 µg/mL streptomycin, and methotrexate for cell selection (wtCFTR-CHO: 100 µM, G551D-CHO: 20 µM, pNUT-CHO: 20 µM) (Tabcharani et al., 1991; Becq et al., 1994). The human pulmonary epithelial cell line Calu-3 cell (American Type Culture Collection) (Shen et al., 1994) was maintained in DMEM-Ham's F-12 (1:1) nutritive mix supplemented by 10% FBS and 100 IU/mL penicillin and 100 µg/mL streptomycin (Dérand et

al., 2004). The human nasal epithelial JME/CF15 cell line, derived from a F508del homozygous patient (Jefferson et al., 1990) was maintained in DMEM-Ham's F-12 (3:1) nutritive mix supplemented by 10% FBS, 100 IU/mL penicillin and 100 µg/mL streptomycin, 5 µg/mL insulin, 5 µg/mL transferrin, 5.5 µM epinephrine, 180 µM adenine, 1.64 nM EGF (Epidermal Growth Factor), 2 nM T3 (3,3′,5-Triiodo-L-thyronine Sodium salt) and 1.1 µM hydrocortisone (Norez et al., 2006). All culture media and antibiotics were from Gibco BRL (Invitrogen, Cergy-Pontoise, France), FBS was from Perbio (PerbioScience, Brebières, France). Hormones and growth factors were from Sigma. Cells were seeded in 24-well plates for iodide efflux and [cAMP] measurements, and in 35-mm plastic dishes for whole-cell patch clamp recordings. Medium was renewed at 2-day intervals.

[cAMP] measurements. Calu-3 cells were incubated for 5-10 min at 37°C in culture medium with drugs at indicated concentration. Supernatants were collected and cells lysed with TCA 12%. The different collected fractions were homogenized and centrifuged. The cAMP was evaluated with RIA ^{125}I-cAMP kit (PerkinElmer Life Sciences, Courtaboeuf, France). The radioactivity was counted by gamma Cobra II counter (Perkin Elmer). The cAMP values were determined following the manufacturer instructions.

Iodide efflux. Screening of small molecules and concentration-response curves were determined by measuring the rate of iodide (^{125}I) efflux with a high capacity robotic system (MultiProbe II EXT, PerkinElmer Life Sciences, Courtaboeuf, France) adapted to the determination of iodide efflux as previously described (Marivingt-Mounir et al., 2004). Our protocol of screening is as follows. Four different cell types, wtCFTR-CHO, G551D-CFTR CHO, Calu-3 and CF-15 were incubated in multiwell plates at 37°C in Krebs solution containing 1 µM KI and 1 µCi Na^{125}I/ml (NEN, Boston, MA) during 30 min (CHO cells) or 1

JPET Fast Forward. Published on July 7, 2006 as DOI: 10.1124/jpet.106.104521
This article has not been copyedited and formatted. The final version may differ from this version.

h (Calu-3 and CF15 cells) to permit the ^{125}I to reach equilibrium. The first three aliquots were used to establish a stable baseline in cold Krebs buffer (from t_0 to t_2). A medium containing the appropriate drug was then used for the remaining aliquots from t_3 to t_8. Residual radioactivity was extracted at the end of the experiment with a mixture of 0.1 N NaOH and 0.1% SDS, and determined using a gamma counter (Cobra II, PerkinElmer Life Sciences, Courtaboeuf, France). The fraction of initial intracellular ^{125}I lost during each time point was determined and time-dependent rates (k = peak rate, min^{-1}) of ^{125}I efflux calculated from the following equation: $k = \ln (^{125}I_{t1} / {}^{125}I_{t2})/ (t_1 - t_2)$, where $^{125}I_t$ is the intracellular ^{125}I at time t, and t_1 and t_2 are successive time points (Marivingt-Mounir et al., 2004). Relative rates were calculated: k_{peak}-k_{basal} (min^{-1}), i.e. the maximal value for the time-dependent rate (k_{peak}, min^{-1}) excluding the third point used to establish the baseline (k_{basal}, min^{-1}). Concentration-dependent activation curves were constructed as % of maximal activation (set at 100%) transformed from the calculated relative rates. In some experiments, chloride transport inhibitors were present in the loading solution and in the efflux buffer. The activity of CFTR-dependent iodide efflux was stimulated either by 1 µM forskolin or by pyrrolo[2,3-*b*]pyrazines derivatives or by a cocktail containing 1 µM forskolin + pyrrolo[2,3-*b*]pyrazines. Other details are elsewhere (Marivingt-Mounir et al., 2004).

Whole-cell patch clamp recordings. Whole-cell patch clamp experiments were performed on Calu-3 and wtCFTR-CHO-cells at room temperature. Currents were recorded with a RK-400 patch-clamp amplifier (Biologic, Grenoble, France). I-V relationships were built by clamping the membrane potential to –40 mV and by pulses from –80 mV to +80 mV (20 mV increments). Pipettes with resistance of 3-4 MΩ were pulled from borosilicate glass capillary tubing (GC150-TF10, Clark Electromedical Inc., Reading, UK) using a two-step vertical puller (Narishige, Japan). They were filled with the following solution: 1 mM NaCl, 113 mM

JPET Fast Forward. Published on July 7, 2006 as DOI: 10.1124/jpet.106.104521
This article has not been copyedited and formatted. The final version may differ from this version.

L-Aspartic Acid, 113 mM CsOH, 1 mM $MgCl_2$, 27 mM CsCl, 1 mM EGTA, 10 mM TES, 3 mM MgATP (pH 7.2; 285 mOsm). They were connected to the head of the patch-clamp amplifier through an Ag-AgCl pellet. Seal resistances ranging from 6 to 20 GΩ were obtained. Results were analysed with the pClamp 6.0.2 package software (pClamp, Axon Instruments). The external bath solution contained 145 mM NaCl, 4 mM CsCl, 1 mM $CaCl_2$, 1 mM $MgCl_2$, 10 mM glucose and 10 mM TES (pH 7.4; 340 mOsm with mannitol). The liquid potential was corrected before seal establishment. Pipette capacitances were electronically compensated in cell-attached mode. To standardize experiments, recordings were performed only when the input resistance has a value ≤10 MΩ. The mean value of access resistance was 7.3 ± 1.1 MΩ (n = 7) for Calu-3 cells and 7.9 ± 0.8 MΩ (n = 5) for wtCFTR-CHO cells. Membrane capacitances were measured in the whole-cell mode by fitting capacitance currents, obtained in response to a hyperpolarisation of 6 mV, with a first-order exponential and by integrating the surface of the capacitance current. Mean values of membrane capacitance were 52.2 ± 12.2 pF (n = 7) for Calu-3 cells and 63.7 ± 11.6 pF (n = 5) for wtCFTR-CHO-cells. For graphic representations, I-V relationship was normalized to 1 pF, in order to remove variability due to differences in cell sizes. For time-course experiments, current amplitude measured at +40mV was plotted each 15 seconds.

Short-circuit current measurement. Experiments were carried out on the colon epithelium of wild-type (*Cftr*$^{+/+}$) or CFTR knock-out (*Cftr*$^{-/-}$) mice B6 129-CFTR^{tm1Unc} (Snouwaert et al., 1992) obtained from CNRS-CDTA (centre de distribution, typage et archivage animal, Orléans, France). Animals were killed by cervical dislocation, a procedure approved by the local animal ethic committee of the University of Poitiers. We use one animal per experiment (N is the number of animals). The ascending colon was removed, opened longitudinally and washed in ice-cold PBS. The muscle layers and connective tissue were dissected away from

the colon epithelium. The epithelium was mounted in a vertical Ussing chamber (Harvard Apparatus, Holliston MA, USA; 0.26 cm² surface area). Luminal and serosal sides were bathed at 37°C with a nutrient buffer containing (in mM) 120 NaCl, 1.2 $CaCl_2$, 1.2 $MgCl_2$, 0.8 K_2HPO_4, 3.3 KH_2PO_4, 25 $NaHCO_3$, 10 D-Glucose. The pH of this solution was 7.4 when gassed with 95% O_2 - 5% CO_2 at 37°C. The upper level of fluids in both luminal and serosal reservoirs was identical. After mounting tissues in Ussing chamber, an equilibration period ≥ 40 min was allowed for stabilization of basal electrical properties. Transepithelial potential difference (V_{TE}) was measured by the Ag/AgCl electrodes placed as close as possible to (and on either side of) the epithelium, in order to reduce the magnitude of the solution series resistance. They were connected to the preamplifier headstage of an amplifier (EC-825 Epithelial Voltage-Clamp, Warner Instruments Corporation, Hamden CT, USA). Potential difference values were corrected for the junction potential between the luminal and serosal solutions when no tissue was mounted in the chamber. The polarity of I_{sc} and V_{TE} was referred to serosal side of the epithelium. An apical anion secretion was indicated by a decrease in I_{sc}. Transepithelial resistances (R_{TE}) were determined according to Ohm's law, from the voltage deflection (ΔV_{TE}) due to pulsed current injection (1 sec) of 0.5 µA and subtraction of the empty chamber resistance. In our experiments, the range of colonic epithelia R_{TE} was 580-2000 $\Omega.cm^{-2}$ and the means were 1113 ± 157 $\Omega.cm^{-2}$ (N = 20) for *Cftr*$^{-/-}$ mice colon and 1388 ± 251 $\Omega.cm^{-2}$ (N = 26) for wild-type mice colon (no significant difference). Data were collected with the Chart V.4.2.2 package software (ADInstruments Phy Ltd, Castle Hill, Australia). All experiments were carried out in the presence of amiloride (500 µM) in the apical solution in order to prevent sodium transport.

Data analysis. All the data are presented as mean value ± SEM, where n refers to the number of experiments and N to the number of animals. For the I_{sc} experiments and iodide efflux

experiments, the unpaired student's t-test was used to compare sets of data, whereas for [cAMP] measurements, the paired student's t-test was used (duplicate experiments). All graphs are plotted with GraphPad prism 4.0 for Windows (GraphPad Software, San Diego, CA, USA). Values of $P<0.05$ were considered as statistically significant: * $P<0.05$, ** $P<0.01$, *** $P<0.001$. Non significant (ns) difference was $P>0.05$.

JPET Fast Forward. Published on July 7, 2006 as DOI: 10.1124/jpet.106.104521
This article has not been copyedited and formatted. The final version may differ from this version.

Results

Our study was carried out with the 12 pyrrolo[2,3-*b*]pyrazines derivatives shown in Fig. 2A. These agents are named RP derivatives (see table 1) to facilitate the reading. These compounds were selected from a library of more than 100 derivatives synthesized in our laboratory because they share structural determinants with other CFTR activators (reviewed in Becq, 2006).

Identification of cAMP-independent CFTR activators. We first examined the effects of 100 µM of each compound on CHO cells stably expressing wtCFTR with our robotic cell-based primary screening assay using iodide efflux measurement. This assay allowed the rapid detection of CFTR channel activity from cells cultured in 24-well plates. Several control experiments have been first performed on resting cells (noted ctrl for control, corresponding to 0%) or on cells stimulated with a submaximal concentration (1 µM) of the adenylate cyclase activator forskolin (hereafter noted fsk, corresponding to 100%, grey bar in Fig. 2B). This minimal concentration of fsk was chosen because it allows low stimulation of CFTR-dependent iodide efflux as previously reported (Marivingt-Mounir et al., 2004). Among these compounds only 7-*n*-butyl-6-(4-hydroxyphenyl)[5*H*]pyrrolo[2,3-*b*]pyrazine *(*RP-107) and 7-*n*-butyl-6-(4-chlorophenyl)[5*H*]pyrrolo[2,3-*b*]pyrazine (RP-108) activated an iodide efflux above the control (Fig. 2B). The remaining 10 RP compounds did not stimulate iodide efflux (dashed line in Fig. 2B was set at the level of fsk response). To begin to characterize the mechanism of activation, we determined the cellular cAMP level in wtCFTR-CHO cells in the following experimental conditions: with cells stimulated by 1 µM fsk alone or stimulated by 1 µM fsk plus 100 µM RP-107 or plus 100 µM RP-108 and with cells stimulated by 10 µM fsk. Fig. 2C shows that neither RP-107 nor RP-108 potentiated the cAMP level measured

JPET Fast Forward. Published on July 7, 2006 as DOI: 10.1124/jpet.106.104521
This article has not been copyedited and formatted. The final version may differ from this version.

with 1 μM fsk alone. In addition, the compounds alone have no effect on the basal cellular cAMP level.

Then, we determined the concentration-response relationships in presence of 1 μM fsk plus increasing concentrations of each RP in wtCFTR-CHO cells (Fig. 3). The iodide secretion peaked and then fell rapidly. For RP-107, the peak rate (k_{peak}) of iodide efflux occurred within the first two minutes after adding the compound. In control condition (DMSO), k_{peak} was 0.065 ± 0.003 min^{-1}, in presence of 1 μM fsk, k_{peak} increased to 0.108 ± 0.005 min^{-1} and was significantly potentiated to 0.22 ± 0.008 min^{-1} after the addition of 100 μM RP-107 (n = 4 for each condition). The decline of the efflux rate could be attributed either to tracer depletion (due to a finite source of ^{125}I at the beginning of each experiment), local ATP depletion or desensitization. With 1 μM fsk present, the maximal stimulation (plateau) was achieved at 3 μM (Fig. 3A & 3B) and the half-maximal effective concentration was EC_{50} = 152 ± 1.2 nM for RP-107 (Fig. 3B). For RP-108, the corresponding EC_{50} value was much higher (24 ± 1.2 μM, Fig. 3C). No stimulation in presence of either RP-107 or RP-108 was noted with mock-CHO cells, i.e. non-expressing CFTR cells (not shown). Thus, RP-107 selectively stimulates CFTR-dependent iodide efflux with submicromolar concentrations whereas its analogue RP-108 appears ≈158-fold less potent.

In the following experiments we determined the pharmacological profile for inhibition of the RP-stimulated iodide efflux in wtCFTR-CHO cells. The peak of iodide efflux stimulated by 1 μM fsk + 1 μM RP-107 (k_{peak} = 0.207 ± 0.003 min^{-1}, n = 8) was fully abolished by 100 μM glibenclamide (k_{peak} = 0.063 ± 0.003 min^{-1}, n = 8) and 10 μM $CFTR_{inh}$-172 (k_{peak} = 0.055 ± 0.003 min^{-1}, n = 8), two well-known CFTR inhibitors (Fig. 4A, right traces). In contrast, fsk/RP-107 response was not affected by 100 nM TS-TM calix[4]arene (k_{peak} = 0.2 ± 0.004 min^{-1}, n = 8) or 500 μM DIDS (k_{peak} = 0.213 ± 0.011 min^{-1}, n = 8), two non-CFTR channel inhibitors (Fig. 4A, left traces). A summary of the data is presented Fig.

JPET Fast Forward. Published on July 7, 2006 as DOI: 10.1124/jpet.106.104521
This article has not been copyedited and formatted. The final version may differ from this version.

4B with statistical analysis. Then, we determined the effect of RP-107 in Calu-3 cells, a model for human airway epithelial cells endogenously expressing wtCFTR (Shen et al., 1994; Dérand et al., 2004). Fig. 5A shows stimulation by RP-107 of iodide efflux in Calu-3 cells in the absence of fsk. As can be seen in Fig. 5A, the latency to reach the maximum efflux response (k_{peak}) was reduced at higher RP-107 concentrations (t_5 at 100-300 nM but t_3 at 1-10 µM). The corresponding half-maximal effective concentration was EC_{50} = 303 ± 1.5 nM (n = 4, Fig. 5B right). In similar experiment but in the presence of submaximal concentration of fsk (1 µM), RP-107 activated the efflux with a greater affinity (EC_{50} = 140 ± 2.6 nM, n = 4, Fig. 5B left). These results suggest that the stimulation of CFTR by RP-107 depends on the phosphorylation state of the channels.

Activation of G551D- and F508del-CFTR by RP-107. To determine whether RP-107 could activate CFTR mutants, we performed iodide efflux experiments with cells expressing two of the most common CF mutations, i.e. the class III mutation G551D-CFTR studied with CHO cells stably expressing G551D-CFTR and the class II deletion F508del-CFTR studied in human airway epithelial CF15 cells endogenously expressing F508del-CFTR protein. The mutation G551D-CFTR disrupts activation of CFTR and phosphorylation alone is not able to achieve sufficient stimulation of G551D-dependent Cl^- transport (Welsh & Smith, 1993; Becq et al., 1994; Illek et al., 1999; Marivingt-Mounir et al., 2004). Iodide efflux experiments on G551D-CFTR CHO cells have been performed in the presence of 10 µM fsk. No stimulation of iodide efflux was found with 10 µM fsk alone (Fig. 6A). However, RP-107 stimulates an efflux in G551D-CFTR expressing cells with an EC_{50} of 1.5 ± 1.1 nM in the presence of 10 µM fsk (n = 4, Fig. 6A). The latency to reach the maximum efflux response (t_5-t_6) was delayed as compared to wild-type CFTR (see Fig. 5). This delay in response may be related to the gating defect of the G551D-CFTR channel (Welsh & Smith, 1993) and to its inability to

JPET Fast Forward. Published on July 7, 2006 as DOI: 10.1124/jpet.106.104521
This article has not been copyedited and formatted. The final version may differ from this version.

response to high concentration of cAMP-agonists (Becq et al., 1994; Illek et al., 1999; Marivingt-Mounir et al., 2004). To study F508del-CFTR we used the human airway epithelial CF15 cells. Prior to the experiments, CF15 cells were incubated 24 hours at low temperature in order to rescue F508del-CFTR from ER retention (Denning et al., 1992), a manoeuvre allowing efficient rescue of functional F508del-CFTR in CF15 cells (Norez et al., 2006). RP-107 stimulates F508del-CFTR with EC_{50} of 111 ± 2.2 nM in presence of 1 µM fsk (Fig. 6B). The latency to reach the maximum efflux response in this case was not delayed like for G551D-CFTR but was similar to that of wild-type CFTR (t_3 for wt-CFTR and F508del-CFTR). Interestingly no stimulation of iodide efflux by 100 µM RP-107 was obtained in CF15 cells cultured at 37°C (control: k_{peak} = 0.11 ± 0.010 min^{-1}, n = 4; RP-107: k_{peak} = 0.13 ± 0.011 min^{-1}, n = 4).

Activation of a linear Cl^- current by RP-107 and inhibition by CFTR inhibitors in Calu-3 and wtCFTR-CHO cells. The iodide efflux data were complemented by whole-cell patch clamp recordings to characterize the effect of RP-107 in Calu-3 and wtCFTR-CHO-cells. To eliminate non-CFTR Cl^- currents (for example outwardly rectifying Cl^- currents), we performed all experiments in presence of 100 nM TS-TM calixarene and 200 µM DIDS in the bath. Fig. 7 presents typical whole-cell currents and associated current-voltage plots (Fig. 7D) recorded in the presence or absence of RP-107 in the bath. In control experiments with unstimulated Calu-3 cells (noted control Fig. 7A), a small linear current was recorded with a current density of 1.2 ± 0.5 pA/pF at +40mV. The addition of 1 µM RP-107 to the bath stimulated a time-independent, non-rectifying current (Fig. 7B) with a reversal potential of -40 ± 0.9 mV (n = 7), close to the theorical Nernst potential equilibrium E_{Cl} of -41mV (Fig. 7D). The current density of the linear Cl^- selective current activated by RP-107 was 11.2 ± 2.7 pA/pF (n = 7, measured at +40mV). The amplitude of the current was statistically different

JPET Fast Forward. Published on July 7, 2006 as DOI: 10.1124/jpet.106.104521
This article has not been copyedited and formatted. The final version may differ from this version.

from the basal current (P<0.001). In the absence of DIDS/calixarene in the bath, 1µM RP-107 stimulated similar linear Cl^- selective current with a current density of 10.2 ± 1.7 pA/pF, not significantly different from experiments including inhibitors.

To further demonstrate that the chloride current activated by RP-107 was due to CFTR, we added 100 µM glibenclamide to the bath after stable and maximal activation of the current (Fig. 7C). The current density significantly decreased in the presence of glibenclamide to 3.1 ± 1.5 pA/pF (P<0.001 compared to RP-107 alone and ns compared to control, Fig. 7D). Whole-cell patch clamp experiments were also conducted in wtCFTR-CHO cells. As expected, RP-107 also stimulated CFTR currents. An example of the concentration- and time-dependent activation of CFTR Cl^- currents (representative of 5 separate cells) is presented in Fig. 8. As for Calu-3 cells we incubated the cells in a mixture of calixarene/DIDS (control in Fig. 8A). In this basal condition the current amplitude was 103 pA at +40mV. Increasing the concentrations of RP-107 in the bath from 10 nM to 10 µM activated a linear Cl^- current (Fig. 8B) with an amplitude (at +40mV) of 309 pA at 10 nM, 633 pA at 100 nM, 1077 pA at 1 µM (Fig. 8A). At 1 µM RP-107 the CFTR Cl^- current was maximal; with 10 µM the current amplitude remained unchanged (1064 pA at +40mV). The current was fully and rapidly (140 pA at +40mV after 2 min) inhibited after the addition to the bath of 10 µM $CFTR_{inh}$-172 (in the presence of 10 µM RP-107). Fig. 8B presents the corresponding time-course of activation for the current traces shown in Fig. 8A. These results show that in wt-CFTR CHO and Calu-3 cells, RP-107 activates CFTR Cl^- currents inhibited by $CFTR_{inh}$-172 and glibenclamide.

Stimulation of the Cl^- secretion in the proximal colon of CFTR wild-type mice but not of CFTR null mice. Finally, we measured the effects of RP-107 and RP-108 on transepithelial ion transport in the mouse colon under short-circuit condition as described in material and methods section. In short-circuited colon of *Cftr*$^{+/+}$ mice (Fig. 9A) the application of 500 µM

JPET Fast Forward. Published on July 7, 2006 as DOI: 10.1124/jpet.106.104521
This article has not been copyedited and formatted. The final version may differ from this version.

amiloride inhibited the resting Na^+ current set by the activity of the amiloride-sensitive ENaC channels (DeJonge et al., 2004). After the serosal application of 10 µM fsk, ΔI_{sc} increased by 19 ± 3.6 $\mu A.cm^{-2}$ (N = 7) which corresponds to Cl^- secretion. After stable stimulation, the current was inhibited by glibenclamide (N = 7). In contrast, with *Cftr*$^{-/-}$ mice whereas the application of 500 µM amiloride also inhibited the resting Na^+ current in short-circuited colon, the serosal application of 10 µM fsk did not have any effect on I_{sc} (ΔI_{sc} = 0.3 ± 0.11 $\mu A.cm^{-2}$, N = 4). No effect of 500 µM glibenclamide was observed (N = 4, Fig. 9B).

The experiments described below were conducted after inhibition of the ENaC current by 500 µM amiloride. Addition of RP-107 to either apical and basolateral, or basolateral only, produced the same response in CFTR wild-type mice colon (Fig. 9C). Increasing concentrations of RP-107 induced a change of I_{sc}, like for the fsk-activated I_{sc}, corresponding to an apical Cl^- secretion. The maximal RP-107-dependent response ΔI_{sc} = 7.27 ± 2.4 $\mu A.cm^{-2}$ (N = 8, Fig. 9C) was fully reversed following bilateral application of 1 mM glibenclamide (ΔI_{sc} = 1.16 ± 1.45 $\mu A.cm^{-2}$, N = 8, P<0.001, Fig. 9C) but was not affected by 500 µM DIDS (ΔI_{sc} = 7.47 ± 0.44 $\mu A.cm^{-2}$, N = 3, data not shown). In contrast, in CFTR null mice colon, no change of I_{sc} was obtained with RP-107 used at the same concentrations (N = 8, Fig. 9D). Fig. 9E indicates ΔI_{sc} for each concentration of RP-107 tested on the colon of *Cftr*$^{+/+}$ and *Cftr*$^{-/-}$ mice (N=8 animals for each). We determined an EC_{50} of 89 ± 6 nM for *Cftr*$^{+/+}$ mice (N = 8, Fig. 9F). Similar experiments have been performed in presence of 1 µM fsk to mimic the protocol of iodide efflux experiments. After the addition of amiloride, the tissue was first stimulated by 1 µM fsk and then by RP-107. After stable stimulation by fsk of the apical Cl^- secretion, the response was further potentiated by RP-107 with an EC_{50} of 173 ± 36 nM (N = 6). Finally, with RP-108 we found stimulation of a glibenclamide-sensitive apical Cl^- secretion in *Cftr*$^{+/+}$ but not *Cftr*$^{-/-}$ mice with an EC_{50} of 103 ± 9 µM (N = 6).

JPET Fast Forward. Published on July 7, 2006 as DOI: 10.1124/jpet.106.104521
This article has not been copyedited and formatted. The final version may differ from this version.

Discussion

In the present study we report on the discovery of 6-phenylpyrrolo[2,3-*b*]pyrazines, a novel family of wild-type CFTR, G551D and F508del-CFTR activators. These agents have been identified with our CF drug discovery program using a simple and robust robotic cell-based assay allowing the discovery of small correctors and potentiators of CFTR chloride channels. Two agents are described here: RP-107 and RP-108. RP-107 is the most potent with an affinity of 140-152 nM on wild-type CFTR (Calu-3 and wtCFTR-CHO cells), 1.5 nM on G551D-CFTR and 111 nM on temperature-corrected F508del-CFTR. The Cl^- secretion was stimulated in proximal colon of mice with an affinity of ≈ 90 nM for RP-107 and 103 µM for RP-108. The mechanism of action, although still unknown is independent of cAMP but depends on the phosphorylation state of CFTR because these agents have a greater affinity for the phosphorylated channels. RP-107 and RP-108 are selective for CFTR because in non-expressing CFTR cells (mock-CHO cells), in F508del cells at 37°C (CF15 cells) and in the colon of *Cftr*$^{-/-}$ mice, these agents have no effect on iodide efflux, whole cell Cl^- currents or I_{sc}. Although we have no evidence for a direct activation of CFTR it is reasonable to conclude that 6-phenylpyrrolo[2,3-*b*]pyrazines selectively activate CFTR but not other Cl^- channels.

6-phenylpyrrolo[2,3-*b*]pyrazines (Aloisines). This family of compounds has been first described as cyclin-dependent kinase (CDK) and glycogen synthase kinase-3 (GSK-3) inhibitors (Mettey et al., 2003). Aloisines act by competitive inhibition of ATP binding to the catalytic subunit of the kinases and may be of therapeutic value in Alzeimer's disease since implication of CDK5 and GSK-3 has been suggested in the disease (Knockaert et al., 2002). All the compounds listed in Fig. 2 and tested on CFTR function are active on CDK1, 2 and 5 at submicromolar concentrations (Mettey et al., 2003) but not all of them are CFTR

JPET Fast Forward. Published on July 7, 2006 as DOI: 10.1124/jpet.106.104521
This article has not been copyedited and formatted. The final version may differ from this version.

activators. This indicates that CFTR activation and CDK inhibition are probably not related, which also suggests that the design of a CFTR-specific activator may be achieved after careful determination of the structural determinants of Aloisines.

Structural determinants for CFTR activation. To begin to define a structure-activity relationship with 6-phenylpyrrolo[2,3-*b*]pyrazines tailored to CFTR activation, we compared the chemical structure of RP-107 and RP-108 with the 10 inactive related derivatives (Fig. 2A) and with several known CFTR activators. First within the 6-phenylpyrrolo[2,3-*b*]pyrazines family we observed that RP-108 bearing a 4-chlorophenyl substituent is less potent than RP-107 having 4-hydroxyphenyl substituent. In addition 4-methoxyphenyl compounds (RP-11, RP-95, RP-127, RP-106 and RP-149) are inactive. Therefore one favourable determinant for CFTR activation is the phenyl ring substituted at the 4-position with the following potency OH>Cl>>OCH_3. Interestingly a hydroxyphenyl substituent appears also for NS004, NS1619, genistein, apigenin and MPB compounds (reviewed in Becq, 2006). A chlorine atom is also commonly found for NS004, MPB and 1,2,3,4-tetrahydroisoquinoline-3-carboxylic acid diamides (Gribkoff et al., 1994; Marivingt-Mounir et al., 2004; Hirth et al., 2005). Some agents possess both OH and Cl on the same ring (NS004) or on different rings (MPB-91 and MPB-104). In a previous structure-activity-relationship of the CFTR activators benzo[*c*]quinolizinium salts (Marivingt-Mounir et al., 2004) we observed that alkyl substituent, and especially butyl chain, improved the efficacy of the drugs. Interestingly the substitution of the pyrrolopyrazines core with butyl in R_1 (Fig.1) is also present in RP-107 and RP-108 (Fig. 2A). Therefore a second favourable determinant for CFTR activation is the length of the alkyl chain with the following potency $(CH_2)_3$-CH_3>> H ≈ CH_3 ≈ $(CH_2)_2$-CH_3 ≈ $(CH_2)_4$-CH_3 as found in compounds RP-107, RP-108 >> RP-26 ≈ RP-96 ≈ RP-132 ≈ RP-150. Finally, compounds RP-26 having the OH-phenyl but not the butyl

chain, RP-106 having the butyl chain but not the OH-phenyl or RP-14 having the Cl-phenyl but not the butyl chain are not activators. These observations suggest that both determinants (OH-phenyl and butyl chain) are required for CFTR activation. These very preliminary data provide some interesting clues to improve the potency of future 6-phenylpyrrolo[2,3-*b*]pyrazines.

Towards a new scaffold structure for CFTR activation. The CFTR activators of the first generation were originally identified after investigations of the intracellular signalling pathways (phosphodiesterases and phosphoprotein phosphatases) (reviewed in Becq 2006). This field has profoundly changed the last decade with the achievement of specific and new screening assays developed by universities (Chappe et al., 1998; Galietta et al., 2001; Ma et al., 2002; Yang et al., 2003; Sammelson et al., 2003; Marivingt-Mounir et al., 2004; Szkotak et al., 2004) and biopharmaceutical companies (Hirth et al., 2005; Van Goor et al., 2006).

Several commercial agents like phenanthrolines and benzoquinolines have been reported to activate epithelial Cl^- secretion with EC_{50} from 612 µM to 34 µM (Duszyk et al., 2001; Cuthbert, 2003; Cuthbert & MacVinish, 2003). The 4-chloro-benzo[*f*]isoquinoline has an EC_{50} of 4 µM in Calu-3 cells (Murthy et al., 2005). Introducing a halogen atom (Cl) in position 4, increased the efficacy of the agent as compared to other benzoisoquinolines (Szkotak et al., 2004; Murthy et al., 2005). Similar effect after addition of a halogen atom has been noted earlier for benzoquinoliziniums (Marivingt-Mounir et al., 2004). Other agents were discovered by high throughput screening (Galietta et al., 2001; Ma et al., 2002; Yang et al., 2003; Sammelson et al., 2003), like for example 3-(2-benzyloxyphenyl)isoxazoles and 3-(2-benzyloxyphenyl)isoxazolines (Sammelson et al., 2003). Agents with tetrahydrocarbazol, hydroxycoumarin and thiazolidine core structures reversibly activated CFTR with K_d as low as 200 nM (Ma et al., 2002). Of note, trifluoromethylphenylbenzamine activated G551D-

CFTR channels with a K_d > 10 μM (Ma et al., 2002). Stimulation of F508del-CFTR activity was also reported with tetrahydrocarbazol and N-phenyltriazine with K_d below 1 μM (Ma et al., 2002). Further HTS efforts also identified 1,2,3,4-tetrahydroisoquinoline-3-carboxylic acid diamides as CFTR modulators with nanomolar potency (Hirth et al., 2005) and quinazolinone from a library of 164,000 synthetic compounds (Van Goor et al., 2006).

In conclusion, we have identified 6-phenylpyrrolo[2,3-*b*]pyrazines as a new scaffold structure for the selective activation of CFTR, with submicromolar affinity on wild-type CFTR, G551D- and F508del-CFTR, two of the most common CF mutations. Although the mechanism of activation is still unknown, the challenge will be to design more potent CFTR-specific activators and to determine their potential and optimal use for therapeutic application in cystic fibrosis and CFTR-related diseases.

Acknowledgments: The authors wish to thank Nathalie Bizard, Patricia Léon and James Habrioux for excellent technical assistance, Drs Singh and Bridges for generous gift of TS-TM calix[4]arene and Laurent Meijer for discussions.

References

Anderson MP, Berger HA, Rich DP, Gregory RJ, Smith AE, Welsh MJ (1991). Nucleotide triphosphate are requiered to open the CFTR chloride channel. *Cell* **67**:775-784.

Becq F, Jensen TJ, Chang XB, Savoia A, Rommens JM, Tsui LC, Buchwald M, Riordan JR, Hanrahan JW (1994). Phosphatase inhibitors activate normal and defective CFTR chloride channels. *Proc Natl Acad Sci USA* **91**:9160-9164.

Becq F, Mettey Y, Gray MA, Galietta LJ, Dormer RL, Merten M, Metaye T, Chappe V, Marvingt-Mounir C, Zegarra-Moran O, Tarran R, Bulteau L, Derand R, Pereira MM, McPherson MA, Rogier C, Joffre M, Argent BE, Sarrouilhe D, Kammouni W, Figarella C, Verrier B, Gola M, Vierfond JM (1999). Development of substituted Benzo[*c*]quinolizinium compounds as novel activators of the cystic fibrosis chloride channel. *J Biol Chem* **274**:27415-27425.

Becq F (2006). On the discovery and development of CFTR chloride channel activators. *Curr Pharm Des* **12**:471-484.

Chappe V, Mettey Y, Vierfond JM, Hanrahan JW, Gola M, Verrier B, Becq F (1998). Structural basis for specificity and potency of xanthine derivatives as activators of the CFTR chloride channel. *Br J Pharmacol* **123**:683-693.

Cuthbert AW (2003). Benzoquinolines and chloride secretion in murine colonic epithelium. *Br J Pharmacol* **138**:1528-1534.

Cuthbert AW, MacVinish LJ (2003). Mechanisms of anion secretion in Calu-3 human airway epithelial cells by 7,8-benzoquinoline. *Br J Pharmacol* **140**:81-90.

Davis ML, Wakefield BJ, Wardell JA (1992). Reactions of β-(lithiomethyl)azines with nitriles as rate to pyrrolo -pyridines, -quinolines, - pyrazines, -quinoxalines and pyrimidines. *Tetrahedron* **48**, 939-952.

De Jonge HR, Ballmann M, Veeze H, Bronsveld I, Stanke F, Tummler B, Sinaasappel M (2004). Ex vivo CF diagnosis by intestinal current measurements (ICM) in small aperture, circulating Ussing chambers. *J Cyst Fibrosis* **3**:159-163.

Denning GM, Anderson MP, Amara JF, Marshall J, Smith AE, Welsh MJ (1992). Processing of mutant cystic fibrosis transmembrane conductance regulator is temperature-sensitive. *Nature* **358**:761-764.

Dérand R, Montoni A, Bulteau-Pignoux L, Janet T, Moreau B, Muller JM, Becq F (2004). Activation of VPAC1 receptors by VIP and PACAP-27 in human bronchial epithelial cells induces CFTR-dependent chloride secretion. *Br J Pharmacol* **141**(4):698-708

Duszyk M, MacVinish L, Cuthbert AW (2001). Phenanthrolines, a new class of CFTR chloride channel openers. *Br J Pharmacol* **134**:853-864.

Galietta LV, Jayaraman S, Verkman AS (2001). Cell-based assay for high-throughput quantitative screening of CFTR chloride transport agonists. *Am J Physiol Cell Physiol* **281**:C1734-C1742.

Gray MA, Greenwell JR, Argent BE (1988). Secretin-regulated chloride channel on the apical plasma membrane of pancreatic duct cells. *J Membr Biol* **105**:131-142.

Gribkoff VK, Champigny G, Barbry P, Dworetzky SI, Meanwell NA, Lazdunski M (1994). The substituted benzimidazolone NS004 is an opener of the cystic fibrosis chloride channel. *J Biol Chem* **269**:10983-81096.

Hirth BH, Qiao S, Cuff LM, Cochran BM, Pregel MJ, Gregory JS, Sneddon SF, Kane JL Jr (2005). Discovery of 1,2,3,4-tetrahydroisoquinoline-3-carboxylic acid diamides that increase CFTR mediated chloride transport. *Bioorg Med Chem Lett* **15**:2087-2091.

Illek B, Zhang L, Lewis NC, Moss RB, Dong JY, Fischer H (1999). Defective function of the cystic fibrosis-causing missense mutation G551D is recovered by genistein. *Am J Physiol* **277**:C833-C839.

Jefferson DM, Valentich JD, Marini FC, Grubman SA, Iannuzzi MC, Dorkin HL, Li M, Klinger KW, Welsh MJ (1990). Expression of normal and cystic fibrosis phenotypes by continuous airway epithelial cell lines. *Am J Physiol* **259**:L496-L505.

Knockaert M, Greengard P, Meijer L (2002). Pharmacological inhibitors of cyclin-dependent kinases. *Trends Pharmacol Sci* **23**:417-425.

Ma T, Thiagarajah JR, Yang H, Sonawane ND, Folli C, Galietta LJ, Verkman AS (2002). Thiazolidinone CFTR inhibitor identified by high-throughput screening blocks cholera toxin-induced intestinal fluid secretion. *J Clin Invest* **110**:1651-1658.

Marivingt-Mounir C, Norez C, Derand R, Bulteau-Pignoux L, Nguyen-Huy D, Viossat B, Morgant G, Becq F, Vierfond JM, Mettey Y (2004). Synthesis, SAR, crystal structure, and biological evaluation of benzoquinoliziniums as activators of wild-type and mutant cystic fibrosis transmembrane conductance regulator channels. *J Med Chem* **47**:962-972.

Mettey Y, Gompel M, Thomas V, Garnier M, Leost M, Ceballos-Picot I, Noble M, Endicott J, Vierfond JM, Meijer L (2003). Aloisines, a new family of CDK/GSK-3 inhibitors : SAR study, crystal structure in complex with CDK2, enzyme selectivity, and cellular effects. *J Med Chem* **46**:222-236.

Murthy M, Pedemonte N, MacVinish L, Galietta L, Cuthbert A (2005). 4-chlorobenzo[*f*]isoquinoline (CBIQ), a novel activator of CFTR and DeltaF508 CFTR. *Eur J Pharmacol* **516**:118-124.

Norez C, Antigny F, Becq F and Vandebrouck C (2006). Maintaining low calcium level in the endoplasmic reticulum restores abnormal endogenous F508del-CFTR trafficking in airway epithelial cells. *Traffic* **7**:562-573.

Quinton P (1983). Chloride impermeability in cystic fibrosis. *Nature* **301**:421-422.

Ratjen F and Doring G (2003). Cystic fibrosis. *Lancet* **361**:681-689.

Riordan JR, Rommens JM, Kerem B, Alon N, Rozmahel, Grzelczak Z, Zielenski J, Lok S, Playsic N, Chou JL, et al (1989). Identification of the cystic fibrosis gene: cloning and characterization of complementary DNA. *Science* **245**:1066-1073.

Sammelson RE, Ma T, Galietta LJ, Verkman AS, Kurth MJ (2003). 3-(2-benzyloxyphenyl)isoxazoles and isoxazolines: synthesis and evaluation as CFTR activators. *Bioorg Med Chem Lett* **13**:2509-2012.

Shen BQ, Finkbeiner WE, Wine JJ, Mrsny RJ, Widdicombe JH (1994). Calu-3 : a human airway epithelial cell line that shows cAMP-dependent Cl^- secretion. *Am J Physiol* **266**:L493-L501.

Sheppard DN, Welsh MJ (1999). Structure and function of the CFTR chloride channel. *Physiol Rev* **79**:S23-S45.

Singh AK, Venglarik CJ, Bridges RJ (1995). Development of chloride channel modulators. *Kidney Int* **48**:985-993.

Snouwaert JN, Brigman KK, Latour AM, Malouf NN, Boucher RC, Smithies O, Koller BH (1992). An animal model for cystic fibrosis made by gene targeting. *Science* **257** :1083-1088.

Szkotak AJ, Murthy M, MacVinish LJ, Duszyk M, Cuthbert AW (2004). 4-Chloro benzo[*f*]isoquinoline (CBIQ) activates CFTR chloride channels and KCNN4 potassium channels in Calu-3 human airway epithelial cells. *Br J Pharmacol* **142**:531-542.

Tabcharani JA, Chang XB, Riordan JR, Hanrahan JW (1991). Phosphorylation-regulated Cl^- channel in CHO cells stably expressing the cystic fibrosis gene. *Nature* **352**:628-631.

Van Goor F, Straley KS, Cao D, Gonzalez J, Hadida S, Hazlewood A, Joubran J, Knapp T, Makings LR, Miller M, Neuberger T, Olson E, Panchenko V, Rader J, Singh A, Stack JH, Tung R, Grootenhuis PD, Negulescu P (2006). Rescue of delF508 CFTR trafficking and gating in human cystic fibrosis airway primary culture by small molecule. *Am J Physiol Lung Cell Mol Physiol* **290**:1117-1130.

Vierfond JM, Mettey Y, Mascrier-Demagny L, Miocque M (1981). Cyclisation par amination intramoléculaire dans la série de la pyrazine. *Tetrahedron Lett* **22**, 1219-1222.

Welsh MJ, Smith AE (1993). Molecular mechanisms of CFTR chloride channel dysfunction in cystic fibrosis. *Cell* **73**:1251-1254.

Yang H, Shelat AA, Guy RK, Gopinath VS, Ma T, Du K, Lukacs GL, Taddei A, Folli C, Pedemonte N, Galietta LJ, Verkman AS (2003). Nanomolar affinity small molecule correctors of defective Delta F508-CFTR chloride channel gating. *J Biol Chem* **278**:35079-35085.

Footnotes: This work was supported by the French association Vaincre la Mucoviscidose (VLM), ABCF proteins and CNRS. SN was supported by a thesis studentship from MucoVie 66. CN was supported by a thesis studentship from VLM. CF was supported by a specific grant from CNRS. Part of this work has already been published in an abstract form, in *Pediatric Pulmonology, 2005.*

JPET Fast Forward. Published on July 7, 2006 as DOI: 10.1124/jpet.106.104521
This article has not been copyedited and formatted. The final version may differ from this version.

Figure legends :

Figure 1. Scheme for the synthesis of 6-phenylpyrrolo[2,3-*b*]pyrazines.

Figure 2. Screening of pyrrolo[2,3-*b*]pyrazines derivatives. A, structure of the 12 pyrrolo[2,3-*b*]pyrazines compounds tested (numbered 1 to 12). B, effects of these agents on iodide efflux in wtCFTR-CHO cells. All compounds were tested (n = 4) in presence of 1 µM fsk at 100 µM, except RP-149 and RP-150 (300 µM). The corresponding effect was normalized to that of 1 µM fsk (100%, indicated by the dashed line). C, effect of the 2 active derivatives RP-107 and RP-108 (at 100 µM) on $[cAMP]_i$ of Calu-3 cells in the presence or absence of forskolin at 1 µM and compared to the effect at 10 µM fsk (n = 6 each). ** P<0.01, *** P<0.001. ns, non significant.

Figure 3. Concentration-response relationships for RP-107 and RP-108 on iodide efflux in wtCFTR-CHO cells. A, time-dependent iodide efflux experiments performed in presence of increasing concentrations of RP-107 as indicated. The control is 1 µM fsk. The horizontal bar above traces in A indicates the presence of agonists. Each data point is mean ± SEM of n = 4. In B and C, concentration-response curves for RP-107 and RP-108, respectively. n = 4 for each concentration.

Figure 4. Pharmacological profile of RP-107 induced iodide efflux on wtCFTR-CHO cells. Inhibitors were preincubated 30 min before experiment and iodide efflux was stimulated by 1 µM fsk + 1 µM RP-107. A, effects of 100 nM calixarene, 500 µM DIDS (left traces), 100 µM glibenclamide and 10 µM $CFTR_{inh}$-172 (right traces). Control (ctrl): vehicle only. Each data point is mean ± SEM of n = 8. The horizontal bar above traces in A indicates the presence of

agonists, inhibitors or vehicle (noted control). B, bar graphs of the normalized results obtained in A (n = 8 for each condition). *** P<0.001; ns, non significant.

Figure 5. Stimulation of iodide efflux by RP-107 in Calu-3 cells. A, effect of increasing concentrations of RP-107 on the iodide efflux. The horizontal bar above traces indicates the presence of RP-107 at the indicated concentration. No forskolin present. Each data point is mean ± SEM of n = 4. B, plots of the concentration-response effects of RP-107 alone (right) or RP-107 in presence of 1 µM fsk (left). Each data point is mean ± SEM of n = 4.

Figure 6. Effect of RP-107 on class II and class III CFTR mutants. A, effect of RP-107 in G551D-CFTR CHO cells. Iodide efflux stimulated in presence of increasing concentrations of RP-107 and in presence of 10 µM fsk (left). Plots of the concentration-response effect are presented on the right. B, effect of RP-107 in human airway epithelial F508del-CFTR CF15 cells. Iodide efflux stimulated in presence of increasing concentrations of RP-107 and in presence of 1 µM fsk (left). Plots of the concentration-response effects are presented on the right (each data point is mean ± SEM of n = 4). For the experiments on CF15 cells (F508del-CFTR) cells were incubated 24 hours at low temperature (n = 4 for each condition). The horizontal bar above traces indicates the presence of RP-107 or fsk at the indicated concentration.

Figure 7. Whole-cell patch-clamp experiments performed on Calu-3 cells. All experiments were performed in presence of 100 nM calixarene and 200 µM DIDS in the bath to inhibit non-CFTR chloride channels. A, currents recorded in control condition. B, currents recorded after addition of 1 µM RP-107 to the bath. C, currents recorded after addition of 100 µM glibenclamide to the bath already containing 1 µM RP-107. D, plots of the mean ± SEM

current density/voltage in the three experimental conditions (n = 5 for each). *** P<0.001; ns, non significant compared to control.

Figure 8. Whole-cell patch-clamp experiments performed on wtCFTR-CHO cells. All experiments (n = 5) were in presence of 100 nM calixarene and 200 µM DIDS in the bath to inhibit non-CFTR chloride channels. A, whole-cell chloride currents recorded in control condition, after adding increasing concentrations of RP-107 to the bath from 10 nM to 10 µM as indicated above current traces, or after adding 10 µM $CFTR_{inh}$-172 to the bath already containing 10 µM RP-107. B, corresponding time-course of whole-cell current. Note the presence of calixarene/DIDS during all the experiment and of $CFTR_{inh}$-172 only at the end.

Figure 9. Ussing chamber recordings of I_{sc} in mice ascending colon. A and B, effect of 500 µM amiloride, 10 µM fsk and 500 µM glibenclamide on wtCFTR (A) and wtCFTR null (B) mice colon. C and D, effect of cumulative concentrations of RP-107 and glibenclamide on wtCFTR (C) and wtCFTR null (D) mice colon. In C and D, we first added 500 µM amiloride before increasing concentrations of RP-107 were applied to serosal side of the two types of tissue. Note that glibenclamide was only added on wild-type mice colon. E, effect of RP-107 on the change in I_{sc} (ΔI_{sc}) on wild-type (open bars) or CFTR null (filled bars) mice colon. The change of I_{sc} was defined as a difference of current between the sustained phase of the response and the respective baseline (µA/cm²), for each experiment. Each bar is mean ± SEM (N = 8 for CFTR null mice colon and N = 8 for wild-type mice colon, unpaired experiments). F, corresponding plots of the concentration-response (ΔI_{sc}) for wild-type mice colon. *** P<0.001; ns, non significant.

JPET Fast Forward. Published on July 7, 2006 as DOI: 10.1124/jpet.106.104521
This article has not been copyedited and formatted. The final version may differ from this version.

Table 1

Structure, yields and physical data of compounds **1-12**

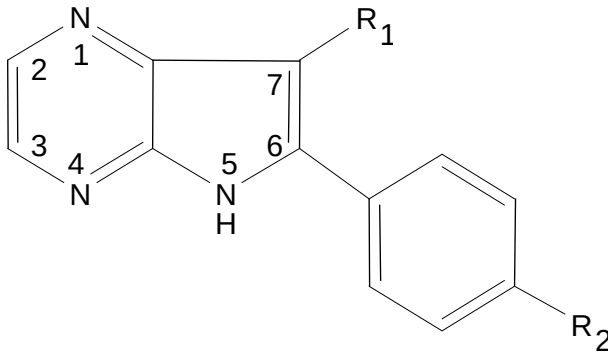

Compound N°	R_1	R_2	Yield (%)	m.p. (°C)	formula
1 (RP11)	H	OCH_3	48	256.1[b]	$C_{13}H_{11}N_3O$
2 (RP26)	H	OH	30[a]	255 dec.	$C_{12}H_{10}N_3OBr$, H_2O
3 (RP95)	CH_3	OCH_3	47	221.6	$C_{14}H_{13}N_3O$
4 (RP96)	CH_3	OH	41[a]	262 dec.	$C_{13}H_{12}N_3OBr$
5 (RP127)	*n*-C_3H_7	OCH_3	26	188.5	$C_{16}H_{17}N_3O$
6 (RP132)	*n*-C_3H_7	OH	50[a]	244 dec.	$C_{15}H_{16}N_3OBr$
7 (RP106)	*n*-C_4H_9	OCH_3	32	183.8	$C_{17}H_{19}N_3O$
8 (RP107)	*n*-C_4H_9	OH	66[a]	281.4	$C_{16}H_{17}N_3O$
9 (RP 149)	*n*-C_5H_{11}	OCH_3	27	144.2	$C_{18}H_{21}N_3O$
10 (RP150)	*n*-C_5H_{11}	OH	74[a]	270.7	$C_{17}H_{19}N_3O$
11 (RP14)	H	Cl	49	250 dec.[c]	$C_{12}H_8N_3Cl$
12 (RP108)	*n*-C_4H_9	Cl	70	200.0	$C_{16}H_{16}N_3Cl$

[a] Calculated from methoxycompounds; [b]238-240°C (Davis et al., 1992); [c] 250°C dec. (Davis et al., 1992).

JPET Fast Forward. Published on July 7, 2006 as DOI: 10.1124/jpet.106.104521
This article has not been copyedited and formatted. The final version may differ from this version.

Figure 1

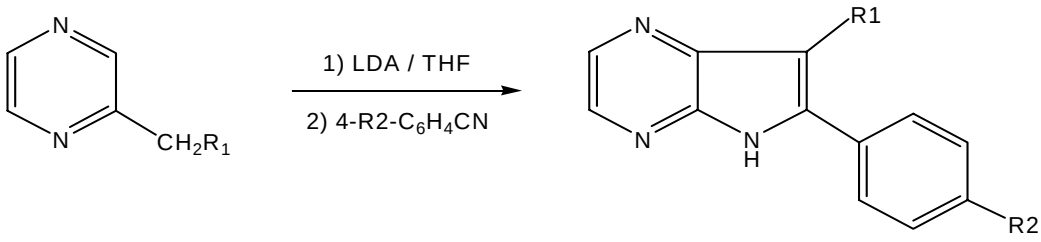

R1 = H, CH_3, *n*-C_3H_7, *n*-C_4H_9, *n*-C_5H_{11}
R2 = OCH_3, Cl

JPET Fast Forward. Published on July 7, 2006 as DOI: 10.1124/jpet.106.104521
This article has not been copyedited and formatted. The final version may differ from this version.

Figure 2

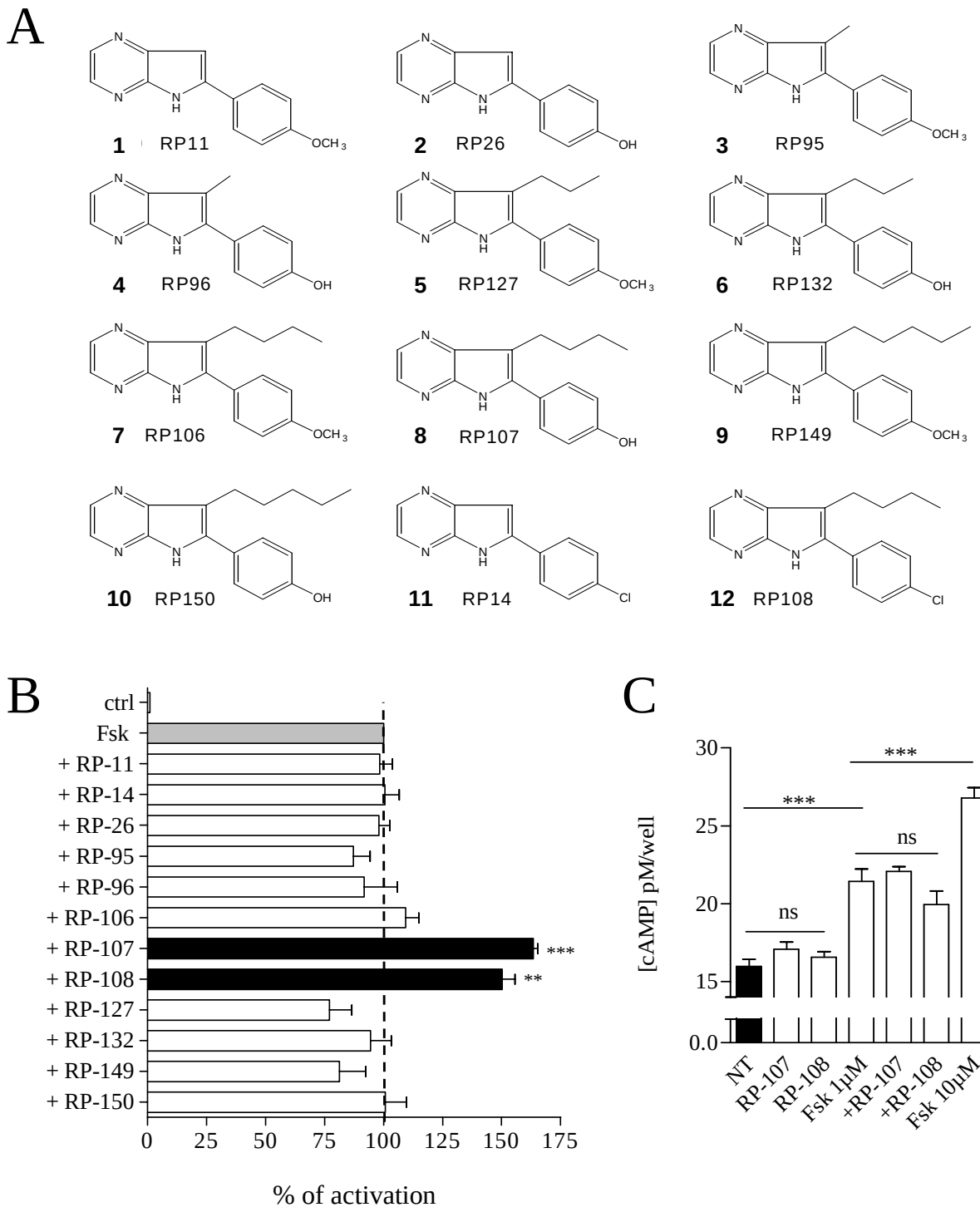

JPET Fast Forward. Published on July 7, 2006 as DOI: 10.1124/jpet.106.104521
This article has not been copyedited and formatted. The final version may differ from this version.

Figure 3

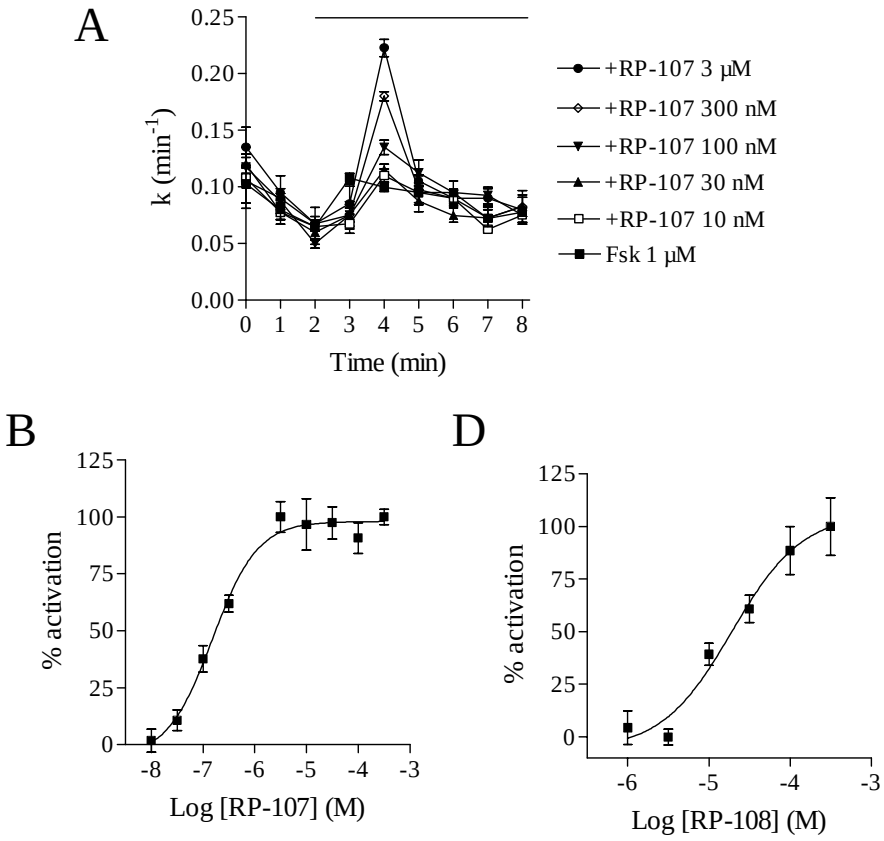

JPET Fast Forward. Published on July 7, 2006 as DOI: 10.1124/jpet.106.104521
This article has not been copyedited and formatted. The final version may differ from this version.

Figure 4

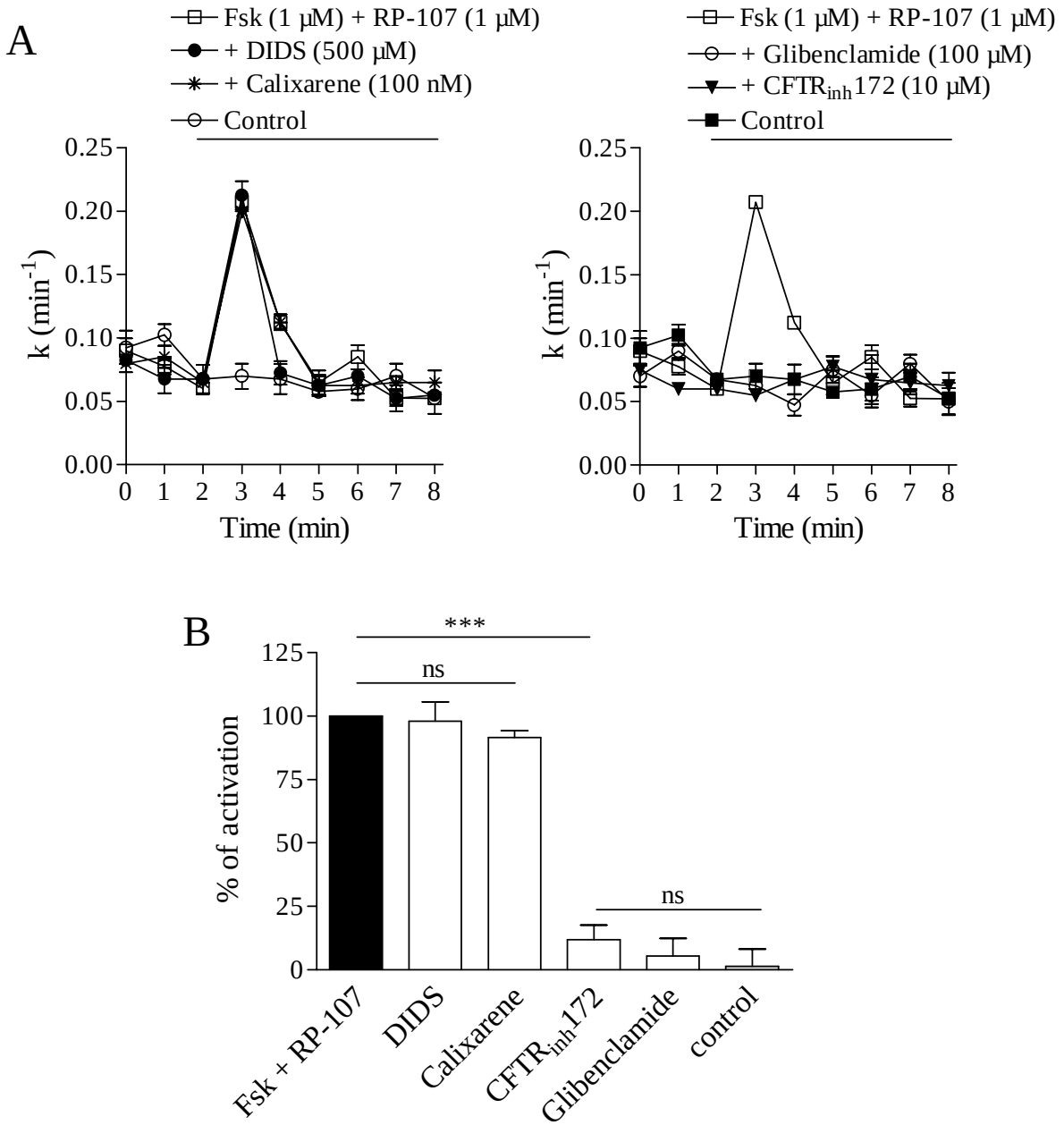

JPET Fast Forward. Published on July 7, 2006 as DOI: 10.1124/jpet.106.104521
This article has not been copyedited and formatted. The final version may differ from this version.

Figure 5

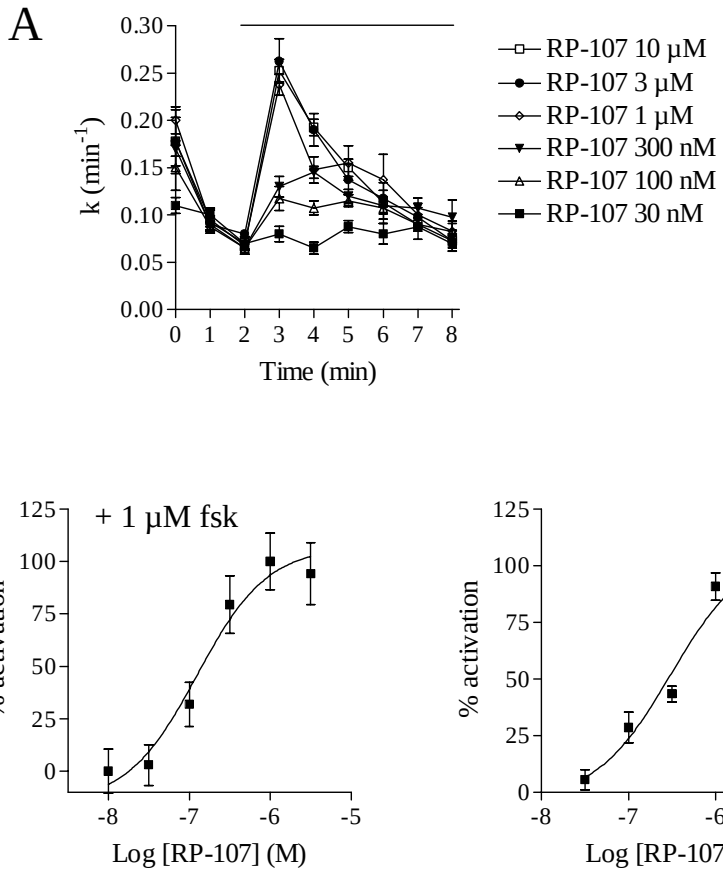

JPET Fast Forward. Published on July 7, 2006 as DOI: 10.1124/jpet.106.104521
This article has not been copyedited and formatted. The final version may differ from this version.

Figure 6

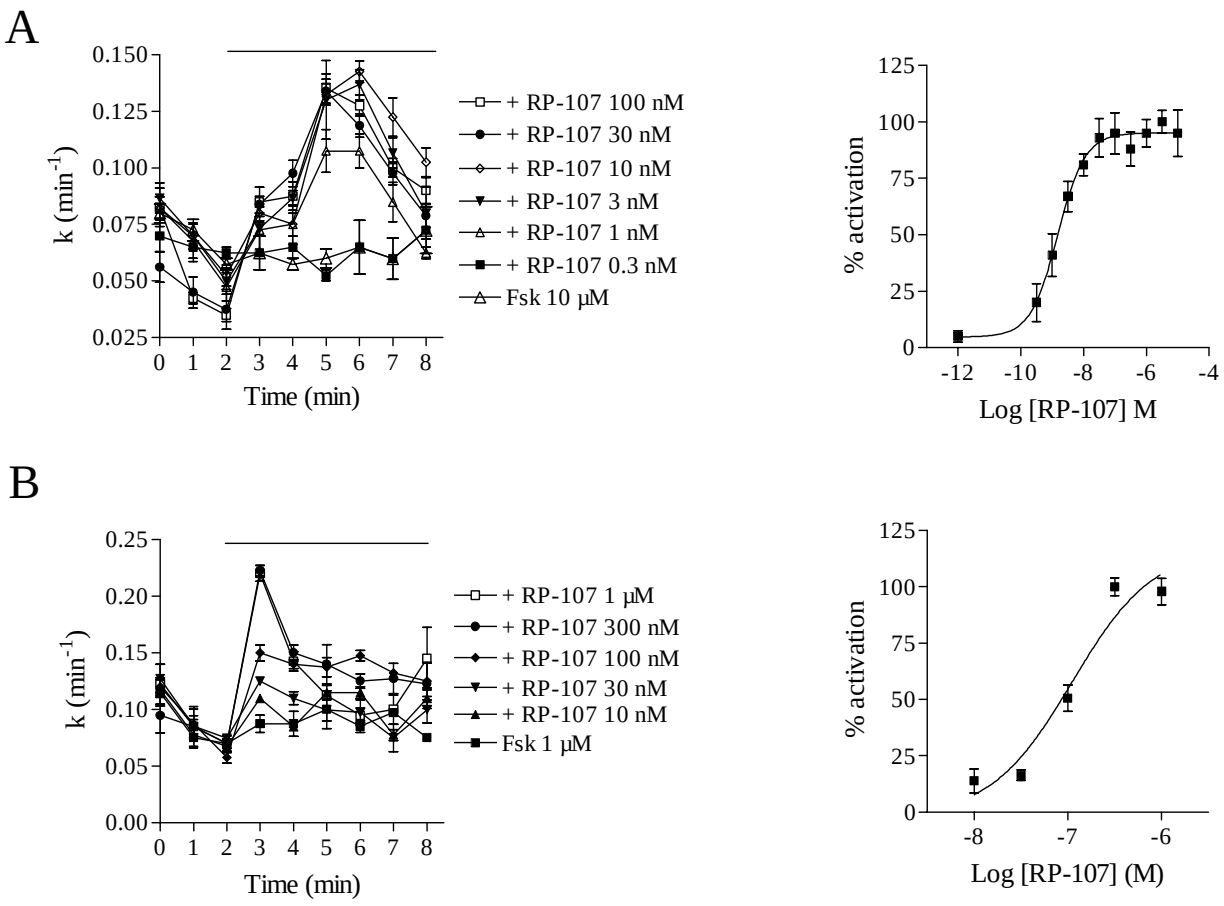

JPET Fast Forward. Published on July 7, 2006 as DOI: 10.1124/jpet.106.104521
This article has not been copyedited and formatted. The final version may differ from this version.

Figure 7

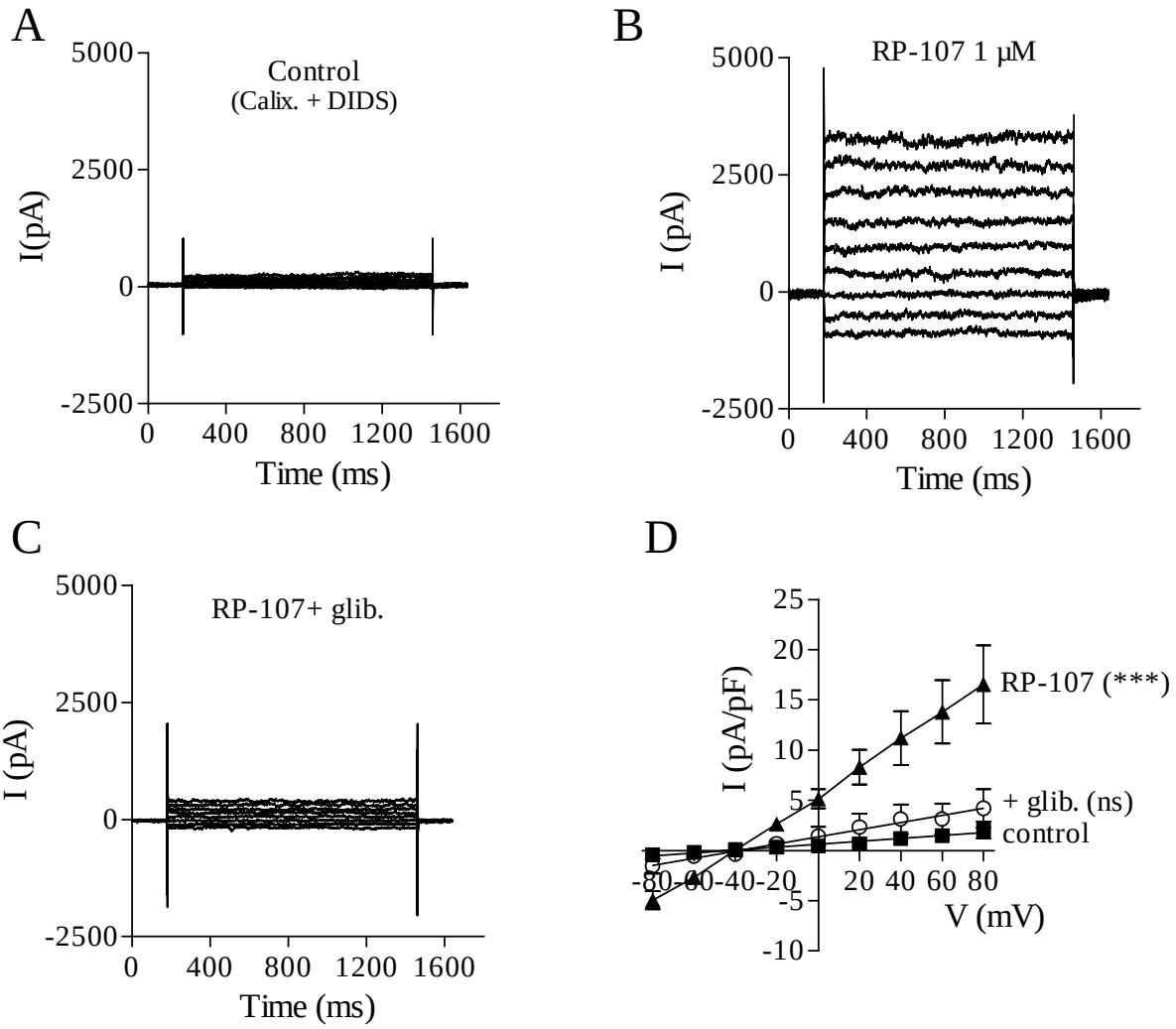

JPET Fast Forward. Published on July 7, 2006 as DOI: 10.1124/jpet.106.104521
This article has not been copyedited and formatted. The final version may differ from this version.

Figure 8

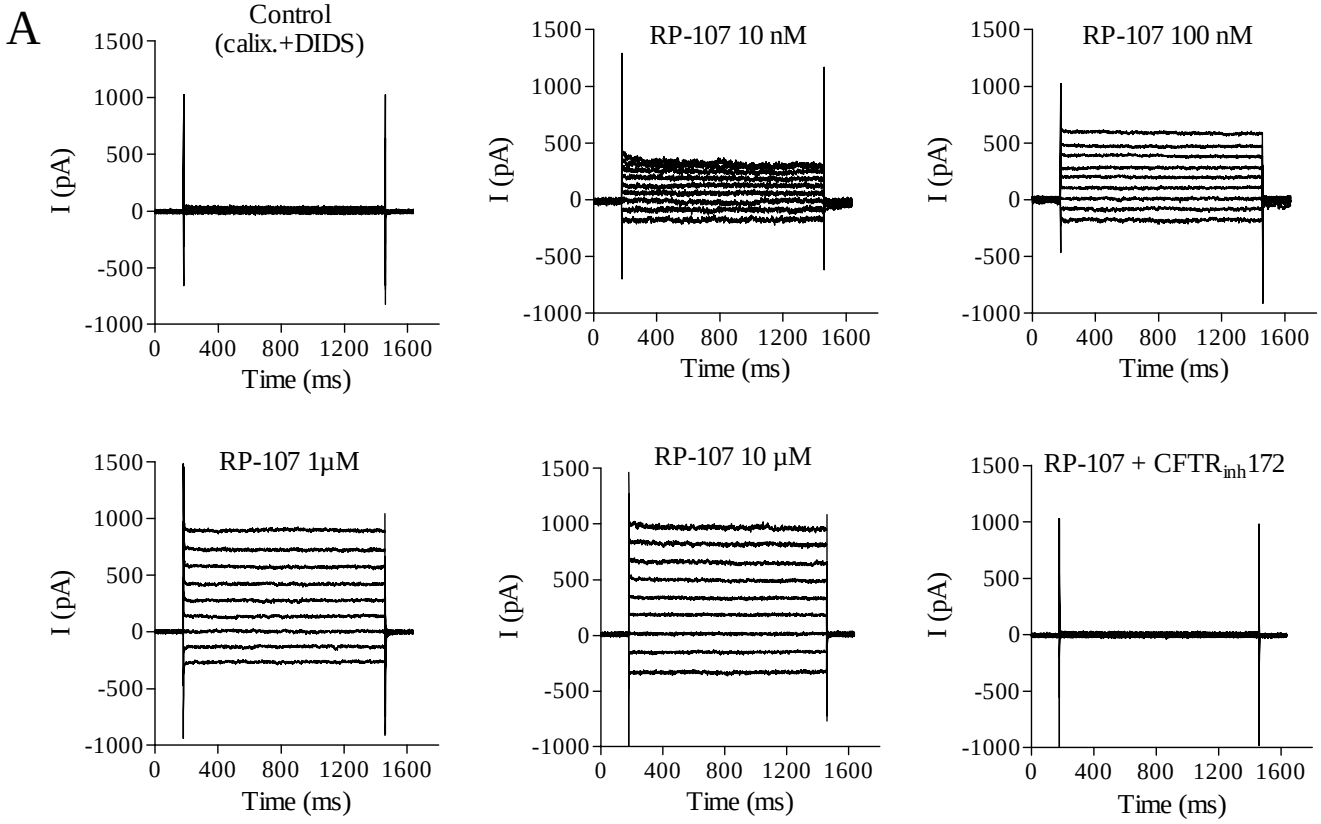

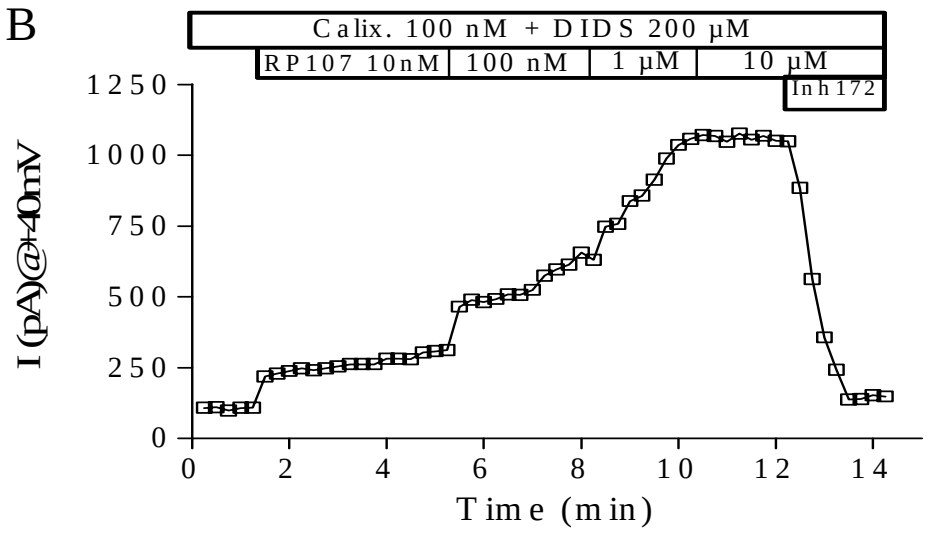

JPET Fast Forward. Published on July 7, 2006 as DOI: 10.1124/jpet.106.104521
This article has not been copyedited and formatted. The final version may differ from this version.

Figure 9